JOURNAL OF GEOPHYSICAL RESEARCH, VOL. 113, G04028, doi:10.1029/2008JG000727, 2008

Click Here for Full Article

Using a horizontal precipitation model to investigate the role of turbulent cloud deposition in survival of a seasonal cloud forest in Dhofar

Anke Hildebrandt[1] and Elfatih A. B. Eltahir[2]

Received 12 March 2008; revised 2 July 2008; accepted 1 October 2008; published 11 December 2008.

[1] This paper investigates a feedback between vegetation height and cloud interception in a seasonal semiarid cloud forest in Dhofar, Oman. In this forest, cloud interception by tree canopies (horizontal precipitation) constitutes a substantial fraction of available water. Owing to cattle browsing on tree canopies the forest is gradually degrading to grassland. We investigated if tree removal could reduce cloud interception to the extent that natural reestablishment of trees is inhibited. For this, we included a model describing turbulent cloud deposition as a module into a dynamic vegetation model. The model allows for estimation of cloud deposition based on cloud properties and dynamically changing vegetation structure. Cloud properties were estimated, using an inverse solution of the cloud deposition model, based on measured precipitation and meteorological data. When applying the model to the Dhofar region, we found that equilibrium vegetation depended on the initial vegetation condition. For most of the range of assumed cloud properties, equilibrium vegetation tended toward grassland, when the initial condition was grassland, and to forest, when the model was initialized with forest. However, the difference between the equilibrium vegetation condition emerging from different initial vegetation types depended on the assumed cloud properties. According to these modeling results, land degradation in this semiarid cloud forest might lead to irreversible destruction of the forest biome.

Citation: Hildebrandt, A., and E. A. B. Eltahir (2008), Using a horizontal precipitation model to investigate the role of turbulent cloud deposition in survival of a seasonal cloud forest in Dhofar, *J. Geophys. Res.*, *113*, G04028, doi:10.1029/2008JG000727.

1. Introduction

[2] Cloud forests are ecosystems that are marked by periods of persistent annual or seasonal cloud immersion. The cloud immersion provides for a special environment in these intriguing forests. From the hydrologic perspective, one process is particularly interesting: the interception of cloud droplets by tree canopies, also called horizontal precipitation. This represents a moisture source in addition to rainfall leading to an increase of available water below the vegetation canopy, as compared to above. While most cloud forests are located in moist regions (i.e., map in *Bubb et al.* [2004]), some have been identified in water-limited environments [*del-Val et al.*, 2006; *Hildebrandt et al.*, 2007; *Hutley et al.*, 1997; *Juvik and Nullet*, 1995], where the water gain provided by horizontal precipitation might become an important source of plant available water. Here, we are interested in the region of Dhofar, Oman (Figure 1), where a localized orographic cloud immersion seems to provide a rufugia for moist vegetation at the desert edge of the Arabian Peninsula. Although cloud immersion occurs only in summer, it provides for a moist enough environment to support a closed canopy broad leaved forest on the slopes of the southern coastal mountain range. In those forests, as a result of horizontal precipitation, water arriving below the canopy was estimated to be roughly twice the amount of rainfall (above the canopy) [*Hildebrandt et al.*, 2007]. Considering that average annual rainfall is only 100–250 mm in this semiarid region, the additional water that the forest collects for itself can be considered substantial, and likely plays an important role in forest survival. Traditionally these forests provide for a number of needs of the local population, one of which is feeding camels. Camel owners would cut branches at the base, bend them to the ground in order to make leaves available for camel feeding. During the last decades, increased wealth has led to increase of livestock and hence land use pressure on this forest. Especially the above mentioned cattle browsing (i.e., feeding on the leaves of trees and shrubs) has led to disappearance of the forest, and turned large parts of the original forest into grassland. This ongoing decrease of tree cover leads at the same time to loss of collecting surface area for cloud droplet interception. How does this change in vegetation cover affect water availability for plants?

[3] Although it seems reasonable to assume that grass intercepts less water than trees, a change of cloud intercep-

[1]Department of Computational Hydrosystems Leipzig, UFZ Helmholtz Centre for Environmental Research, Leipzig, Germany.
[2]Department of Civil and Environmental Engineering, Massachusetts Institute of Technology, Cambridge, Massachusetts, USA.

0148-0227/08/2008JG000727$09.00

Figure 1. Location of the region of interest (circled).

tion with such change in size of the collecting body is not straight forward, due to the nonlinear nature of the process. Horizontal precipitation is predominantly a turbulent process by which cloud droplets are mixed inside the canopy and settle on the vegetation [*Shuttleworth*, 1977]. Generally, droplets can be introduced to the canopy from (1) the side (edge effect) and (2) from aloft (turbulent deposition). Figure 2 depicts both of those processes. The name "horizontal precipitation" is somewhat misleading in that it is figurative only for the edge effect, whereas turbulent deposition is of greater importance for the more frequent closed canopy. In case 1, deposition occurs within short distance from the edge, but deposition is negligible at distance from the edge. For case 2, on the other hand, the source of cloud droplets is within the air aloft, and deposition should be independent of horizontal position, but depend on canopy properties.

[4] Published data on cloud interception over different vegetation types suggest that cloud interception by short vegetation like grass is smaller compared to forest. Unfortunately, a number of variables that influence the results besides flora, such as wind speed, liquid water content (*LWC*) and droplet sizes, complicate comparison of those short period measurements. Eddy covariance and gradient technique measurements have been carried out over both grass and tree cover [*Dollard and Unsworth*, 1983; *Gallagher et al.*, 1992; *Vermeulen et al.*, 1997]. Published cloud droplet deposition maxima were from 0.018 mm/h over grassland [*Dollard and Unsworth*, 1983], 0.021–0.036 mm/h for coniferous forests of different height [*Beswick et al.*, 1991; *Gallagher et al.*, 1992; *Vermeulen et al.*, 1997], and up to 0.4 mm/h over an exposed fir forest [*Lovett*, 1984]. Note that the measurements depend a great deal on the meteorological conditions as stated above.

[5] While observations do not allow for reliable quantification of the change of horizontal precipitation with canopy properties, models do allow for this estimation. *Shuttleworth* [1977] was the first who attempted to develop a model for horizontal precipitation based on turbulent theory. A number of models have followed [*Bache*, 1979; *Lovett*, 1984; *Slinn*, 1982]. Most of them relate horizontal precipitation to wind speed or friction velocity and include some notion of efficiency for particle collection by the canopy. In this work we adopted a version of *Zhang et al.*'s [2001] module for particle deposition for the Canadian Aerosol Model, which is based on the successful model of *Slinn* [1982]. Using this model, allowed us to make predictions of horizontal precipitation based on vegetation and cloud properties. We estimated the cloud properties by inversion of the horizontal precipitation model, making use of a data set gathered in 2003 and 2004 in the cloud forest in Dhofar (Sultanate of Oman) [*Hildebrandt et al.*, 2007]. Coupling of this model to a dynamic vegetation model (Integrated Biosphere Simulator, IBIS [*Foley et al.*, 1996; *Kucharik et al.*, 2000]) allowed us to investigate forest recovery from a degraded landscape. Our results indicate that horizontal precipitation under the degraded landscape (simulated as grassland) is strongly decreased, and is no longer sufficient for survival of a forest biome. A short overview describing the results of this research has already been published [*Hildebrandt and Eltahir*, 2006].

2. Study Site

[6] The area of interest is an isolated deciduous semiarid forest located in the southeast portion of the Sultanate of Oman within a coastal mountain range. The climate is semiarid with a three-monthlong monsoon season (mid June to mid September, locally called khareef). During monsoon, onshore winds from the Arabian Sea push moist air first over a cold upwelling zone offshore the coast [*Currie*, 1992; *Shi*, 2000] and than against the mountain range. This leads to orographic cloud formation and drizzle. The orographic effect leads to dense fog within the mountains that lasts with small interruptions for about three months every year. These mountain ranges are covered with forests. [*Miller and Morris*, 1988]. This lush vegetation forms a narrow max 300–1000m wide and some 300km long green belt that is surrounded by desert [*Kurschner et al.*, 2004]. The forests are thought to be remnant of past

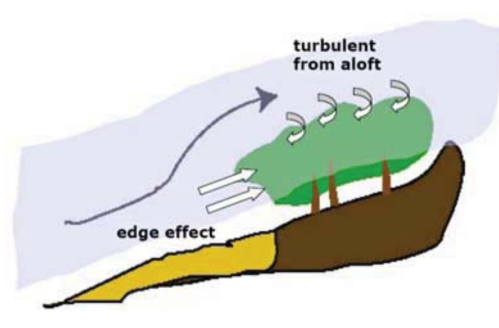

Figure 2. Scheme of horizontal precipitation occurring from aloft through turbulent exchange, and from the side as an edge effect.

moister vegetation belt of paleo-African origin, which almost completely disappeared, when the climate on the Arabian Peninsula changed to the present arid conditions [*Kurschner et al.*, 2004; *Meister et al.*, 2005].

[7] The data used in the following study were collected within this forest by *Hildebrandt et al.* [2007] who give a detailed description of the location. Their research station is located about 450 m above sea level and 20 km away from the coast. Because of the fog conditions, precipitation in this location has two components (1) rainfall and (2) horizontal precipitation (water droplets from the clouds intercepted by the foliage). While rainfall was measured regularly at climate stations, only one study was conducted to quantify net precipitation (rainfall + horizontal precipitation) under natural vegetation in Dhofar [*Hildebrandt et al.*, 2007].

[8] Average annual rainfall from surrounding climate stations ranges from 100 mm (at the coast) to 250 mm (top of the mountain range), including rainfall from cyclones. More than three quarters of the annual rainfall occurs during the monsoon [*Brook and Shen*, 2000], except for years when cyclones occur. Cyclones are exceptional (every 2 to 4 years) but strong events. For example, during a large cyclone on 4–5 June 1989 recorded rainfall was 220 mm, and a smaller cyclone in 2004 led to almost 100 mm rainfall on 30 September 2004. Because of their overwhelming strength these storms contribute a great proportion of the statistical annual average rainfall. However, their influence on the soil water budget seems so be comparatively small, possibly as a result of surface runoff. Soil moisture measurements during the cyclone in 2004 suggest that only shallow soil layers were recharged, while water content in deeper soil layers (60 cm) remained smaller than during monsoon [*Hildebrandt et al.*, 2007].

[9] *Hildebrandt et al.* [2007] determined net precipitation under natural vegetation during the monsoon of 2004 in a location at about half distance between coastal plane and mountain crest. The amount was estimated to be about 295 mm. Using the water budget method, based on rainfall, throughfall and stemflow measurements, they estimated that net precipitation was about twice rainfall above the canopy. Furthermore, about 30% of net precipitation was contributed by stemflow, which appeared to increase infiltration in proximity of the tree trunks. Further, a modeling study by *Hildebrandt and Eltahir* [2007] showed that these drought deciduous forests grow in a marginal, water limited environment, where trees only survive, if most of net precipitation is used for transpiration and all other losses (drainage and grass transpiration) are minimized.

3. Materials and Methods

3.1. Dynamic Vegetation Model

[10] In this research we use a modified version of the Integrated Biosphere Simulator, IBIS [*Foley et al.*, 1996]. The original model is described by *Foley et al.* [1996] and *Kucharik et al.* [2000] with the modifications described by *Hildebrandt and Eltahir* [2007]. The same model was already successfully applied over the same region. It properly reproduced the vegetation type, canopy height, and dynamics of leaf phenology, and soil moisture. Only the most important features of the model are briefly reported here for completeness.

[11] IBIS is a dynamic ecosystem model combined with a Surface Vegetation Atmosphere Transfer (SVAT) scheme. The one-dimensional model is vertically organized in layers, including vegetation layers (upper and lower canopy) and a varying number of soil layers. The vegetation itself is differentiated into Plant Functional Types (PFTs), which are described as either upper (trees) or lower (shrubs, herbs) canopy layer, and in addition differ in leaf form (conifers, broadleaf), leaf habit (deciduous, evergreen) and photosynthetic pathway (C3, C4). Each of the PFTs are assigned a number of physiological parameters and properties, such as rooting profile, the slope of the conductance-photosynthesis relationship, and allocation pattern of carbon within the plant [*Kucharik et al.*, 2000]. Throughout the simulation the PFTs compete with each other for two limited resources: Light and water. Depending on the assigned vegetation properties, the success of securing those resources differs among PFTs and depends strongly on the environment. Nutrient availability is not considered in this version of IBIS.

[12] During any IBIS simulation, a land surface module computes vertical water, energy, momentum and carbon fluxes on an hourly basis. Each day, the phenology module determines the state of deciduous and non-deciduous PFTs according to the season. At the end of the year the carbon balance module integrates the net plant carbon assimilation as the sum of photosynthesis and respiration, and computes the projected or one-sided leaf area index (LAI) as well as biomass for each PFT. The resulting presence or absence of PFTs is a product of competition between PFTs under the prevailing environmental condition.

[13] In the area of interest, stemflow is an important part of the below canopy water balance. Stemflow is a point source of infiltration, and leads to heterogeneous infiltration pattern. Since IBIS is a one dimensional model, it cannot account for heterogeneity in soil moisture. We therefore convert stemflow to a precipitation equivalent, by referring it over a likely infiltration area, as done in the work of *Hildebrandt and Eltahir* [2007].

3.2. Horizontal Precipitation Model

[14] The model addresses two limiting factors that play a role in horizontal precipitation (1) how effectively cloud droplets are transported from the free atmosphere to the surface (2) how effectively the given surface is able to capture and therefore intercept cloud droplets. Models for horizontal precipitation are similar to particle deposition models, with small cloud droplets acting as deposited particles. Therefore, contributions to this field of research originate from the hydrology community as well as from researchers interested in pollutant transport and deposition. Various models for turbulent particle deposition exist, the one by *Slinn* [1982] has been shown to simulate deposition rates that are in good agreement with eddy covariance observations of both particle [*Nemitz et al.*, 2002], and cloud droplet deposition [*Beswick et al.*, 1991]. It is therefore the one that is adopted. According to this model, the flux of cloud droplets from above a canopy (P_{hz}) is described by

$$P_{hz} = LWC \cdot v_d, \tag{1}$$

where v_d is the settling velocity of cloud droplets and *LWC* the cloud liquid water content.

[15] The settling velocity is defined as

$$v_d = c \cdot v_t + v_g, \tag{2}$$

where v_g is the gravitational settling velocity, v_t the turbulent settling velocity, and c is an enhancement factor that accounts for edge effects due to clustering and canopy inhomogeneities. The factor c was added in this work and was not part of the original formulation by *Slinn* [1982], and is defined and discussed below. The factor c is greater or equal to one and describes enhancement of turbulent deposition due to edge effects when the active surface is larger than the horizontal plane that *Slinn*'s [1982] model applies to.

[16] The gravitational settling velocity is the falling velocity of a sphere and depends on the droplet size under consideration. It is calculated as [*Rogers and Yau*, 1996]

$$v_g = \frac{2r_d^2 g \rho_w}{9\eta_a}, \tag{3}$$

where r_d is the cloud droplet radius, g the gravitational constant, ρ_w is the density of water and η_a is the dynamic viscosity of air.

[17] The turbulent deposition is described in analogy with the turbulent transport of momentum (v_m), which is described by

$$v_m = \frac{1}{r_a}, \tag{4}$$

where r_a is the atmospheric resistance

$$r_a = \frac{u_z}{u_*^2} = \frac{\ln\left(\frac{z-d}{z_0}\right)}{\kappa \cdot u_*}, \tag{5}$$

with displacement height, d, roughness length, z_0, friction velocity, u_*, wind velocity, u_z, at a reference height z, and the von Karman constant, κ. In order to define turbulent deposition velocity, equation (5) is modified by introducing an additional resistance called surface resistance, r_{surf}. Thus the turbulent deposition of cloud droplets is given by:

$$v_t = \frac{1}{r_a + r_{surf}}. \tag{6}$$

[18] The surface resistance depends on the efficiency (E) by which a canopy collects cloud droplets of a given size in the following form [*Zhang et al.*, 2001], similar to the formulation of *Slinn* [1982]

$$r_{surf} = \frac{1}{\varepsilon_0 u_* E}, \tag{7}$$

where ε_0 is an empirical constant defined by *Zhang et al.* [2001] who assigned a constant value of 3 for all vegetation types. The same was done here.

[19] The collection efficiency (E) is given by

$$E = E_B + E_{IN} + E_{IM}. \tag{8}$$

[20] The collection efficiency incorporates three processes: Brownian motion E_B, interception by small vegetation hairs (hairs smaller than droplet size), E_{IN}, and impaction efficiency E_{IM}. The latter describes the probability of a particle breaking out of a deviated airflow due to greater inertia, and settling on the deviating object, rather than being carried further within the air stream. For applications that involve particles with typical droplet size, E is dominated by the term E_{IM} [*Slinn*, 1982]. E_{IM} is modeled according to *Zhang et al.* [2001]

$$E_{IM} = \left(\frac{St}{a + St}\right)^2, \tag{9}$$

where St is the Stokes number and a is a vegetation specific parameter, which was defined and tabulated by *Zhang et al.* [2001, Table 3]. The Stokes number is [from *Slinn*, 1982]

$$St = \frac{v_g u_*}{gA}, \tag{10}$$

where A is the characteristic radius or size of the collectors, here the leaves of a specific vegetation type (tabulated in *Zhang et al.* [2001], reproduced in Table 1).

[21] The present model is designed strictly for transport of cloud droplets from aloft into the canopy by means of turbulence, and it does not take into account edge effects. However, in Dhofar forests are clustered, and the top of the canopy is not uniform, but has multiple outcrops. Those outcrops and cluster edges offer an additional surface for droplets to enter the canopy, and observations suggest that horizontal precipitation is enhanced in forest clusters [*Fallas*, 2002]. We account for enhanced precipitation from increased active surface for interaction with the canopy by introducing the enhancement factor c in equation (2). The factor c is defined as the factor by which the horizontal surface (the top) of a tree cluster would have to be multiplied in order to yield the active collection area of the tree cluster (the top plus the sides). To define c we assume that tree clusters have an idealized circular shape with a characteristic radius (R_c). Thus the cluster takes the form of a cylinder with radius R_c; while the height corresponds to the canopy height (h_c) of the trees within the cluster. The active collection area is the surface of the cylinder (except the bottom), while the horizontal area that *Slinn*'s [1982] formulation applies to is only the surface of the top of the cylinder. Therefore, the enhancement factor depends on the canopy height as in

$$c = \frac{2\pi R_c \cdot h_c + \pi R_c^2}{\pi R_c^2} = \frac{2h_c}{R_c} + 1. \tag{11}$$

[22] When the cluster size becomes large as compared to h_c the cluster grows into a forest, in which case $c = 1$ and turbulent deposition is not enhanced. On the other hand, when the characteristic cluster size equals tree height (close to a single standing tree), the enhancement factor $c = 3$. We

Table 1. List of Characteristic Radii of the Collectors (A, Equation (10)) and the Parameter for the Calculation of the Impaction Efficiency (a, Equation (9)) for the Horizontal Precipitation Model[a]

Vegetation Description	IBIS PFT	CAM LUC	A(mm)	a(-)
Tropical Evergreen Forest/Woodland	1	2	5.0	0.6
Tropical Deciduous Forest/Woodland	2	4	5.0	0.8
Temperate Evergreen Broadleaf Forest/Woodland	3	2	5.0	0.6
Temperate Evergreen Coniferous Forest/Woodland	4	1	2.0	1.0
Temperate Deciduous Forest/Woodland	5	4	5.0	0.8
Boreal Evergreen Forest/Woodland	6	2	5.0	0.6
Boreal Deciduous Broadleaf Forest/Woodland	7	4	5.0	0.8
Boreal Deciduous Conifer Forest/Woodland	8	3	2.0	1.1
Mixed Forest	9	5	5.0	0.8
Woody Savanna	10	10	10.0	1.3
Savanna	11	10	10.0	1.3
Grassland	12	6	2.0	1.2
Closed Shrubland	13	10	10.0	1.3
Open Shrubland	14	10	10.0	1.3
Tundra	15	9	-	-
Desert/Barren	16	8	-	-
Polar Desert/Rock/Ice	17	12	-	-
Permanent Wetland	18	11	10.0	2.0

[a]The factors are adopted from *Zhang et al.* [2001], who defined those for different Land Use Categories (LUC) in the Canadian Aerosol Module (CAM). The parameters were reassigned according to IBIS Plant Functional Types (PFTs). In the original formulation the parameter A takes different values for different seasons of the year. Since the cloud immersion period is equivalent with the growing season, the growing season values were selected.

are aware that the clusters usually are not exactly circular. Nevertheless the enhancement factor serves as a simple expression that compares the total active area for horizontal precipitation to the horizontal area through the vegetation height. It allows us to take into consideration the fact that the active area for cloud deposition increases as the height of the vegetation compared to its radius increases. Alternatively to using equation (11), a clustering factor could also be calibrated based on observation. Unfortunately, we do not have sufficient measurements in areas with different clustering to perform a calibration.

[23] Equation (2) shows that the total deposition velocity has contribution from gravitational and turbulent settling. Figure 3 shows the sensitivity of the components of horizontal precipitation (turbulent and gravitational) to droplet radius for vegetation with different height. The gravitational component is solely a function of droplet diameter and will not change with vegetation type. Turbulent deposition, on the other hand, depends on both turbulence and droplet size. Turbulent deposition increases with decreasing atmospheric resistances, therefore, the influence of vegetation itself on turbulent deposition will become most apparent through its surface roughness (z_o, equation (5)). At a given wind velocity, higher deposition rates will be achieved over a rough surface like forest, compared to a relatively smooth surface like grass. Turbulent deposition also increases, when wind velocity increases over a given surface, since this decreases atmospheric resistance (not shown). Finally, when droplet sizes increase gravitational deposition dominates, and turbulent deposition has minor influence on the total deposition. Overall total deposition increases as droplet size increases, but at the same time the influence of surface roughness decreases. In the extreme case droplets would be of raindrop size, turbulent settling velocity would be negligible and total deposition velocity equal to gravitational deposition velocity. The droplets would fall as rain and the vegetation type would have no influence on how much precipitation occurs. Droplet size is therefore an important parameter, when judging the influence of the vegetation cover on horizontal precipitation.

3.3. Integration of the Horizontal Precipitation Model Into IBIS

[24] The horizontal precipitation model was included into IBIS as an additional subroutine. The coupled model will be referred to as IBIS-HZP. The module is run each time step (one hour) and horizontal precipitation is added to the rain. The friction velocity is calculated internally from wind

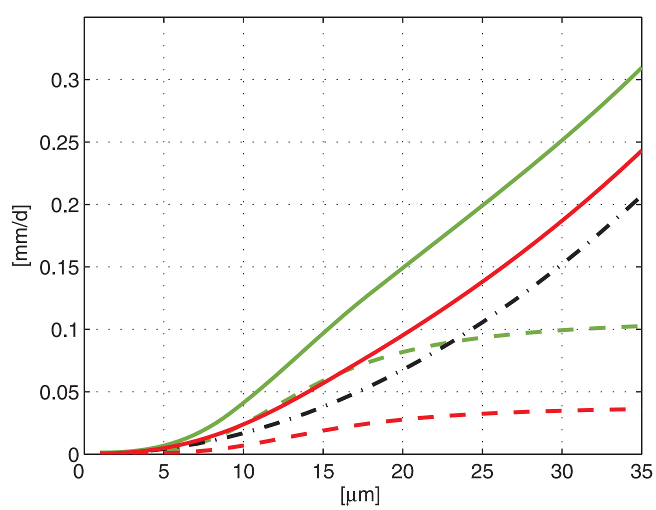

Figure 3. Total settling velocity (solid lines) for cloud droplets and its components, turbulent (dashed) and gravitational settling velocity (dashed dotted, black), plotted as a function of droplet size for two different vegetation types: broadleaf trees with 6.5 m canopy height (green) and grass with 0.5 m canopy height (red). The assumed wind velocity at 30 m above ground was 6 m/s.

Table 2. Derived Cloud Properties of r_d and *LWC* From Inverting a Horizontal Precipitation Model and Assuming an Idealized Canopy With $z_o = 0.1 \cdot h_c$ and $d = 2/3 \cdot h_c$, Where $h_c = 6.5$ m (Measured at the Field Station)

Series Number	c(-)	Cloud Type	r_d(μm)	*LWC*(g m^{-3})
C1	1	Pristine	21.2	0.58
C2	1	Average	15.3	0.96
C3	1	Polluted	12.4	1.43
C4	1.4	Pristine	20.4	0.52
C5	1.4	Average	14.8	0.86
C6	1.4	Polluted	11.9	1.30

speed (input) and the canopy drag coefficient (which changes dynamically according to the mixture of PFTs that make up canopy leaf and stem area). The vegetation parameters (a, A) used in equations (9) and (10) are tabulated in *Zhang et al.* [2001] for the Land Use Categories (LUC) of the Canadian Aerosol Module (CAM). We translated them for IBIS PFTs and listed the values in Table 1.

[25] The clustering factor c was calculated dynamically according to equation (11) and using the canopy height that IBIS simulates and assuming a constant characteristic cluster size of $R_c = 30$ m. Choice of this clustering size is motivated by field observation. Clustering was assumed to be dependent on a minimum tree height of $h_c = 3.5$ m. For trees of lower stature the enhancement factor was assumed to be $c = 1.0$.

4. Model Input

[26] IBIS-HZP is forced with hourly time series of atmospheric boundary conditions (air temperature, rainfall, specific humidity, wind speed, cloudiness, cloud liquid water content (*LWC*) and cloud droplet radius (r_d)).

4.1. Meteorological Input

[27] For all meteorological input except cloudiness and cloud properties we used the data collected during the year 2004 by *Hildebrandt et al.* [2007]. Their hydrological station called Gogub is located in the coastal mountain range of Dhofar (about 17.12°N, 54.6°E), approximately 450 m above sea level and 20 km away from the coast. We use data of the year 2004, which was representative for the average conditions in this region. Missing values in the data set were replaced with those measured during the immediately preceding period. Rainfall above the canopy was not measured in 2004 because of equipment malfunction. However, we estimated rainfall for 2004 based on measurements of throughfall during that year. We used data from 2003 when rainfall and throughfall were measured in parallel and at the same site, to define the relationship between rainfall and throughfall. We found that throughfall was larger by a factor of 1.56 than slope corrected rainfall ($r^2 = 0.69$), and used this relationship to estimate rainfall for 2004. Finally, for simplicity we assume complete cloud cover during the monsoon (mid Jun to mid September) and clear sky condition during the rest of the year, similarly to *Hildebrandt and Eltahir* [2007]. Calculated incoming shortwave radiation based on this assumption agrees well with field measurements.

4.2. Derivation of Cloud Properties

[28] Cloud properties were not measured at the field station. Nevertheless, the horizontal precipitation model requires cloud properties as input. We therefore assumed a range of time constant cloud properties. The choice of pairs of *LWC* and r_d was performed based on two constraints: (1) when running the horizontal precipitation model with this input, it should reproduce the precipitation measured at the field site; (2) the pairs should reflect reasonable and consistent cloud properties, from the perspective of cloud physics. In order to achieve this we relied on the horizontal precipitation model and the parameterization of *McFarquhar and Heymsfield* [2001] for the relation between *LWC* and r_d originally developed for remote sensing applications. We derived pairs of *LWC* and r_d representative of (a) clouds with different numbers of aerosols and (b) canopy types. For cloud types we distinguished (according to equations (4) and (10) [*McFarquhar and Heymsfield*, 2001]): clouds with very few aerosols (for brevity referred to as pristine clouds), average number of aerosols and large number of aerosols (referred to as very polluted clouds, note that the term is not related to anthropogenic influence). For canopy type we differentiated between forest with a closed canopy ($c = 1$), and clustered forest with ($c = 1.4$). The resulting six pairs of *lwc* and r_d are listed in Table 2.

[29] We also derived (not shown) time series of *LWC* and r_d, in order to account for changing cloud properties with time. The procedure is similar to the one described above, except that it is applied not to the entire monsoon, but at each time step. The general modeling result was not sensitive to which input (time constant or time variable) was used [*Hildebrandt*, 2005]. The differences between the six different pairs of *LWC* and r_d provide estimates of the uncertainty in the assumed cloud properties.

5. Performed Experiments

[30] In a first step, we apply the off line horizontal precipitation model to idealized canopies: grass, closed canopy forest and forest cluster. This experiment allows us to judge the difference of horizontal precipitation under different vegetation and cloud properties, achieved with this model.

[31] Second, we run IBIS-HZP with dynamic vegetation, thus allowing the vegetation cover to adapt to the current environment. We run the model on one grid cell of undefined size. Like most SVAT schemes, IBIS considers only vertical fluxes, which are normalized over 1 m^2. Therefore, the size of the grid cell does not need to be defined. The applicable scale is about 10 to some hundred meters. In this experiment we initialized the model once with tree cover (deciduous trees, LAI = 2.0) and once with grass cover (C3 and C4 grasses both initialized with LAI = 2.0). As a spin-off we run the model with static (prescribed) initial vegetation for the first 100 years, and after that the simulation continued with dynamic vegetation (as described above).

[32] All experiments were repeated for all six input pairs (C1–C6) of cloud properties. All other variables were the same, including soil type (sandy loam) and rooting depth (2 m). We used the model input for one single year and repeated it for the length of the simulation. Models were run until vegetation reached equilibrium (year to year change of

Table 3. Results From the Forward Simulation Using the Offline Horizontal Precipitation Model and the Derived Cloud Input From Table 2 Over Different Idealized Canopies With $z_o = 0.1{\cdot}h_c$, $d = 2/3{\cdot}h_c$ and h_c as Indicated[a]

Scenario	Series Number	Cloud Type	h_c (m)	c (-)	Tot Prec (mm)	Rain (mm)	Tot HZP (mm)	HZP Grav (mm)	HZP Turb (mm)
Trees no cluster	**C1**	**Pristine**	**6.5**	**1.0**	**295**	**125**	**170**	**83**	**87**
	C2	**Average**	**6.5**	**1.0**	**295**	**125**	**170**	**70**	**100**
	C3	**Polluted**	**6.5**	**1.0**	**295**	**125**	**170**	**70**	**100**
	C4	Pristine	6.5	1.0	266	125	141	67	74
	C5	Average	6.5	1.0	264	125	139	61	78
	C6	Polluted	6.5	1.0	264	125	139	60	79
Trees 30 m cluster	C1	Pristine	6.5	1.43	337	125	212	83	129
	C2	Average	6.5	1.43	342	125	217	70	147
	C3	Polluted	6.5	1.43	342	125	217	70	147
	C4	**Pristine**	**6.5**	**1.43**	**295**	**125**	**170**	**67**	**103**
	C5	**Average**	**6.5**	**1.43**	**295**	**125**	**170**	**61**	**109**
	C6	**Polluted**	**6.5**	**1.43**	**295**	**125**	**170**	**60**	**110**
Grass	C1	Pristine	0.5	1.0	235	125	110	83	27
	C2	Average	0.5	1.0	227	125	102	70	32
	C3	Polluted	0.5	1.0	227	125	102	70	32
	C4	Pristine	0.5	1.0	220	125	95	67	28
	C5	Average	0.5	1.0	215	125	90	61	29
	C6	Polluted	0.5	1.0	215	125	90	60	30

[a]Changed were h_c, a, and A (to reflect a tree or grass canopy) and the enhancement factor for clustering (c, equation (11)) for tree clusters. Bold indicates the control cases (i.e., cases for which the cloud properties were inversely derived); by definition they yield the observed precipitation (170 mm horizontal, 295 mm total). All precipitation fluxes are indicated as annual cumulated depths.

LAI does not follow a trend, but fluctuates around a constant value); this was always achieved after the performed 1000 yearlong simulations.

6. Results

6.1. Derived Cloud Properties

[33] Table 2 shows the derived droplet radii and *LWC* for three different clouds with varying number of condensation nuclei (pristine, average and polluted clouds) and based on a homogenous and clustered canopy. Table 3 (bold lines) shows the corresponding components of precipitation. Generally, in polluted clouds, smaller droplets and larger *LWC* produce the same horizontal precipitation as (a smaller number of) larger droplets and smaller *LWC* in pristine clouds. Derivation of cloud droplets over a cluster leads to a decrease of both cloud droplets size and *LWC*.

[34] The change in droplet size and *LWC* becomes most apparent in the breakdown of total horizontal precipitation into turbulent and gravitational component. Because of their smaller droplets polluted clouds display a smaller gravitational component, and larger turbulent component than pristine clouds. Since the influence of vegetation is only through the turbulent component, the change of vegetation cover will be more strongly felt in polluted than in pristine clouds. This will also become clearer later, when these cloud types are used in the coupled IBIS-HZP.

6.2. Difference of Horizontal Precipitation Between Closed Canopy Forest, Tree Clusters, and Grasses

[35] Table 3 gives some idea on how vegetation cover influences turbulent deposition and hence total available water in this model. It shows the prediction of the precipitation components based on the developed horizontal precipitation model using the generated input series C1–C6 and measured wind speeds for 2004 over different idealized canopies (homogenous forest, clustered trees and homogenous grass). For these calculations we used the module offline, thus the vegetation is static, and drag was estimated based on displacement height ($d = 2/3{\cdot}h_c$) and roughness length (and $z_o = 0.1{\cdot}h_c$).

[36] Turbulent deposition over grass is about a factor of three smaller compared to a closed canopy forest and about a factor of four smaller compared to a clustered forest. Taking into account the gravitational component and rain, the total precipitation over grass is decreased by 20–28% compared to closed canopy and by 28–33% compared to a clustered canopy. This implies a substantial loss of available water for plants, given that in this area water is already strongly limiting plant growth.

[37] By definition, turbulent deposition over a clustered forest is c times larger than over a closed canopy forest. For a cluster of size of 30 m and a canopy height of 6.5 m (characteristic of the field site), the additional water gain on total precipitation is about 13%.

6.3. Horizontal Precipitation Feedback From a Coupled Model IBIS-HZP

[38] The top panels in Figure 4 show an example of the evolution of LAI (upper and lower canopy) for cloud properties C6, when initialized with forest (Figure 4a) and grass (Figure 4b), respectively. The lower panels (Figures 4c and 4d) give the corresponding annual precipitation, as well as contribution from turbulent and gravitational settling. The rougher tree cover (Figures 4a and 4c) produces larger turbulent cloud deposition, and produces sufficient total precipitation (300 mm) to maintain the forest. For the grass cover, on the other hand, turbulent deposition, and thus total precipitation are much decreased, and hence the more water demanding trees cannot equally develop.

[39] Table 4 gives a summary of all model experiments C1–C6. The upper six rows show the results of experiments with initial conditions for trees, and the lower six rows show experiments that had grassland as the initial condition. For all simulations that were started with forest, the equilibrium vegetation is also forest. The resulting tree cover is drought

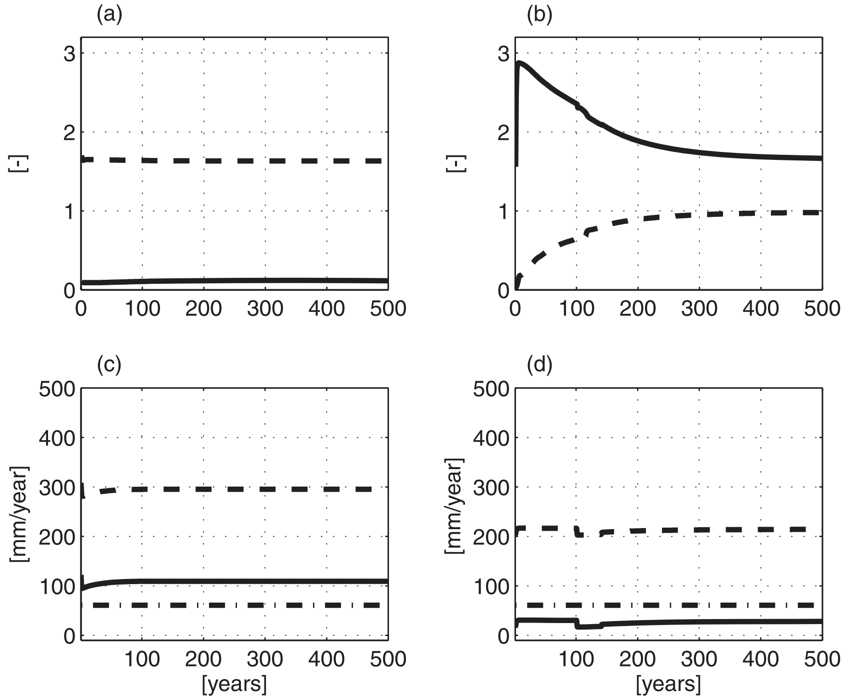

Figure 4. Development of the model (a, b) LAI and (c, d) water fluxes for the first 500 years of the simulation with cloud properties C6, and initial condition forest (Figures 4a and 4c) or grassland (Figures 4b and 4d). Legend: annual LAI of trees (dashed) and grasses (solid) (Figures 4a and 4b); annual cumulated total precipitation (P_{tot}, dashed), annual cumulated contribution from gravitational settling (dashed dotted), and from turbulent settling (solid) (Figures 4c and 4d).

deciduous forest as present at the field site in Gogub, where the data were collected. The modeled tree cover is taller (8.5–8.7 m) than at the field site (6.5 m) but within the range of tree heights elsewhere in the region. The resulting total precipitation is close to the expected 295 mm, with cloud types C1–C3 showing higher precipitation than C4–C6.

[40] With one exception (C1), all simulations that were started with initial condition of grass land, result in open woodland, and display lower tree LAI than cases initialized with forest. In four (C3–C6) out of six cases grass dominates. The total precipitation is much decreased. In one case (C1) the initial condition had no influence on the modeling result (see discussion).

[41] To a certain degree, forests can recover from a degraded state. Figure 5 shows the development of tree LAI for cloud properties C6. Depending on the initial condition, the model produces two distinct equilibria, a forest state and open woodland. Up to an initial tree LAI of 1.8, the vegetation tends to recover to the forest equilibrium. On the other hand an initial tree LAI of 1.6 is no longer maintained, but trees are further degraded toward the

Table 4. Results of the Model Experiments With IBIS-HZP, Using the Cloud Properties Given in Table 2[a]

	Initial		Last Year of Simulation						
Series Number	LAI grass (-)	LAI trees (-)	LAI grass (-)	LAI trees (-)	h_c (m)	Tot Prec (mm)	Tot HZP (mm)	HZP Grav (mm)	HZP Turb (mm)
C1	0.1	2.2	0.09	1.67	8.6	319	194	83	112
C2	0.1	2.2	0.08	1.68	8.7	326	201	70	131
C3	0.1	2.2	0.07	1.69	8.7	336	211	70	141
C4	0.1	2.2	0.15	1.61	8.3	282	157	67	90
C5	0.1	2.2	0.11	1.63	8.4	295	170	61	109
C6	0.1	2.2	0.10	1.64	8.5	303	178	60	117
C1	2.2	0.1	0.09	1.67	8.6	319	194	83	112
C2	2.2	0.1	1.03	1.27	6.5	240	115	70	45
C3	2.2	0.1	1.31	1.16	6.0	230	105	70	35
C4	2.2	0.1	1.33	1.15	5.9	229	104	67	37
C5	2.2	0.1	1.65	0.98	5.1	214	89	61	29
C6	2.2	0.1	1.77	0.92	4.7	209	84	60	23

[a]The top part shows simulations initialized with deciduous trees, and the lower part shows simulations initialized with grassland. Initial LAIs and annual values for the last year of the simulation (1000 years for all simulations) are given. Shown are annual LAI, tree height (h_c), annual accumulated total precipitation (Tot Prec), total annual horizontal precipitation (Tot HZP) and contributions from gravitational (HZP Grav) and turbulent deposition (HZP Turb). The total annual precipitation includes rainfall (125 mm).

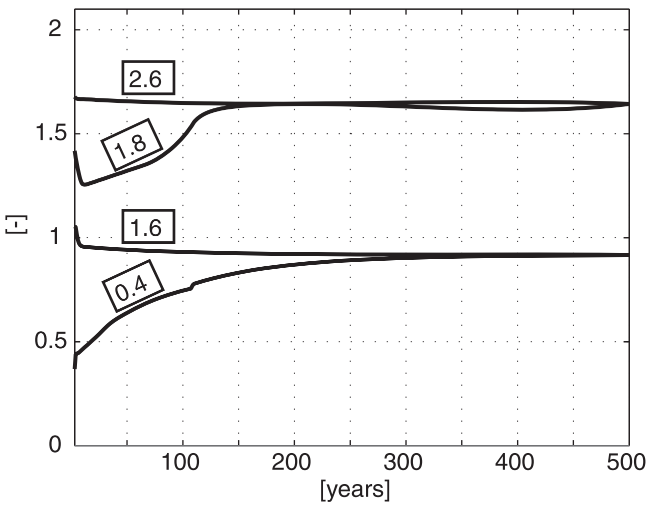

Figure 5. Modeled time evolution of annual tree LAI for various initial tree LAI (indicated in the boxes above the graphs) and cloud properties C6, for the first 500 years of the simulation.

woodland equilibrium. This is representative of all cloud properties, except C1.

7. Discussion

[42] For this model, we find that the system has two stable equilibria, thus the initial condition determines the resulting equilibrium vegetation. This was true except in one case (C1) in which the horizontal precipitation yielded from the assumed forcing for cloud properties was sufficient for tree growth, independent of the initial condition. In general, trees will be of lower stature and have lower LAI when they emerge from grass cover than when they emerge from tree cover. In most of the considered cases where a system was initialized with grassland, tree LAIs were lower at equilibrium than for the corresponding case where the initial condition was trees.

[43] The reason for this bimodal equilibrium is the dependence of friction velocity on the canopy structure. Because trees are taller than grass, they produce a higher surface roughness and trees therefore gain higher total precipitation. In the medium to long-term, in order to maintain biomass necessary for their tall structure (stems and branches in addition to LAI), trees need to provide a higher level of productivity than grasses. Since Carbon uptake is related to transpiration, trees require transpiring more than grasses, and they depend on the additionally gained water from horizontal precipitation in order to achieve the necessary level of productivity to maintain their tall structure. Thus the observed vegetation equilibrium is based on a feedback between the canopy size (i.e., tree height, LAI) on the one hand and the water that the trees are able to gain from this structure on the other. The system will not be in equilibrium as long as the maintenance of the stand structure requires more or less water than can be gained at the current transpiration. This is confirmed by Figure 5.

[44] It is important to note that this equilibrium does not only depend on the tree structure, but also a great deal on the cloud properties. Generally, more distinct equlibria were modeled for the derived polluted cloud properties than for pristine cloud properties. In particular, for cloud property C1 (pristine cloud) only one equilibrium exists. The reason is that series C1 has a higher contribution from gravitational settling, and consequently higher total precipitation over grassland than all other cloud input. Therefore, enough water was available for transpiration at the initial condition (grassland) to allow for trees to emerge

[45] Unfortunately no field observation of cloud properties in Dhofar exist so far, and it is also difficult to confirm cloud properties with measurements at other sites, since they depend a great deal on the local cloud formation process. For example, comparison with cloud properties measured elsewhere indicate that the derived droplet radii cover the expected range, while the cloud liquid water contents are very high [*Dollard and Unsworth*, 1983; *Eugster*, 2006; *Vermeulen et al.*, 1997; *Gallagher et al.*, 1992, 2002]. On the other hand, our derived cloud properties compare well with sites that are characterized by similarly dense orographic cloud formation, which generally tends to create particularly high cloud liquid water contents. Liquid water contents in orographic clouds have been shown to be elevated when the cloud base is very low [*Wieprecht et al.*, 2005], for mountain ridges (as opposed to single mountains) and probably also when mountain outcrops are located downwind of the site [*Hallberg*, 1997], all of which is the case for the field site in Dhofar. In the Great Dunn Fells Experiment 1993, at site, where a mountain range leads to orographic formation of pristine clouds, the cloud liquid water content was measured to 0.4–0.8 g m^{-3} [*Hallberg*, 1997], which compares well with the properties for pristine clouds derived here. Therefore, also given the extremely low visibility during the monsoon (within the range of some 10s of meters), we conclude that at least the cloud liquid water content for pristine and average clouds is realistic (i.e., series C1, C2, C4, C5). The derived liquid water contents for polluted clouds (C3, C5) are high, and would need to be confirmed. While we have no direct field observation about cloud types in Dhofar, pristine clouds are the most unlikely case. Such clouds only form at far distance from land, while the clouds in Dhofar are of marine origin, but formed close to the coast, and within close proximity of the desert. Thus, dust particles will enhance the number of available aerosols. For the Dhofar region we therefore expect clouds with medium to high pollution levels.

[46] Our results indicate that for most cloud type scenarios, two vegetation equlibria exist, one for forest and one for grass, while it is unlikely that forests regrow from the degraded state. The cloud oasis in Dhofar are remnants of a former moister vegetation, which was forced into climatically favored regions in the southern part of the Arabian Peninsula [*Kurschner et al.*, 2004]. One of those are the monsoon affected mountain ranges, where the cloud presence delimits the extent of the forests [*Miller and Morris*, 1988]. Our research indicates that the magnitude of cloud deposition depends on the vegetation, in that enough water to maintain forests can only be gathered under the prerequisite that the forests are already present. This highlights the

risk this semiarid cloud forest is subjected to as a result of camel browsing. These results might be applicable to other semiarid cloud forests in the world, or areas with dense fog, where vegetation is in a grass equilibrium. Generally, such a feedback is only expected in water limited cloud forests, where horizontal precipitation (and particularly the turbulent fraction thereof) provides for a large part of the water balance, and where water demand is at least temporary elevated (here at the end of the monsoon season).

[47] To our knowledge this is the first process based model dedicated to estimating horizontal precipitation for different vegetation types, besides the model of *Walmsley et al.* [1996]. In their model however, horizontal precipitation is reduced to an edge effect on the canopy topography, and turbulent deposition is not resolved. The model presented here, most closely resembles the dry deposition scheme for aerosols proposed by *Zhang et al.* [2001], but is adapted to particles of cloud droplet size. The model can easily be expanded to yield spatial predictions, if meteorological input and cloud properties are available or can reasonably be estimated.

[48] We adopted the horizontal precipitation model according to *Slinn* [1982] with parameterization for vegetation in SVAT models by *Zhang et al.* [2001]. *Slinn*'s [1982] model has been shown to perform successfully in a number of field studies both for particle and fog deposition [*Beswick et al.*, 1991; *Nemitz et al.*, 2002]. However, *Gallagher et al.* [2002] showed a dependency of E_{IM} on the roughness of the surface for small particles ($r_d < 0.12$ μm), which would be of particular interest when modeling the influence of vegetation roughness. Unfortunately, no research is published on particles in the cloud droplet size range ($r_d = 1-25$ μm). *Gallagher et al.* [2002] summarized that for the time being expressions for impaction efficiencies could be used, which are based on specific vegetation types, like the expression by *Zhang et al.* [2001] that was adopted here.

[49] The main deficiency of the model is that a logarithmic wind profile is implied in the derivation of the equations (i.e., atmospheric resistance in equation (5)). Most sites (including the field site in Gogub) do not fulfill the requirements necessary for the application of a logarithmic wind profile, which applies to areas with an infinite uniform surface, and under neutral conditions. Here, we consider a field site located in a forest patch and on top of a hill. Under those circumstances the real wind profile may be considerably different from the idealized logarithmic profile assumed. However, the model is meant to give an idea of the sensitivity of horizontal precipitation to vegetation cover. It cannot resolve all the details of the complex mechanism of horizontal precipitation in Gogub. More detailed models, which resolve turbulence on a small scale, are necessary to estimate the influence of non-idealized canopies on horizontal precipitation. Such an approach can only be applied to very small areas and also requires additional, detailed measurements. Here, we accounted for non-ideal conditions (clustered canopies) by including the clustering factor c in this model. More sophisticated approaches will definitely improve the prediction. Further advanced models could also address additional feedbacks, which were neglected here, such as the role of vegetation change for aerosol abundance and cloud properties.

[50] All in all, our model yields realistic total precipitation and vegetation at equilibrium condition (deciduous forest and open woodland) both of which are landscapes observed in Dhofar. The modeled tree heights for the forest equilibrium are up to 2 m higher than the measured ones at the field site, where the meteorological data were collected. The reason might either be that the model uses generic vegetation parameters, and not specific ones for the endemic tree species at the field site, which are unknown. On the other hand, the trees in the field site are subject to cattle browsing, which might have hampered their growth. Thus, we expect tree stature to be smaller than optimal in the field. The modeled tree heights are within the range of tree heights observed in the area of this species (up to 12 m tall [*Miller and Morris*, 1988]).

8. Conclusion

[51] Here, we developed a horizontal precipitation (HZP) model and tested what influence the vegetation cover would have on horizontal precipitation. Since we did not measure cloud properties at our field site in Gogub (Dhofar, Oman) we estimated those properties. We inverted the horizontal precipitation model and used horizontal precipitation as estimated from measurements at a field station as input to predict cloud properties as output. We derived altogether 6 pairs of cloud properties (droplet radius and cloud liquid water content), based in different assumptions of aerosol abundance and vegetation clustering.

[52] The derived cloud properties were than used as input for forward simulations of the horizontal precipitation model and with varying vegetation to investigate the sensitivity of the model to vegetation type. This investigation showed that (1) grass cover yielded 20–33% less total precipitation than the trees, depending on the cloud properties used, and (2) the assumed cloud properties have great influence on the role of vegetation cover on horizontal precipitation, with pristine clouds leading to smaller changes than polluted ones.

[53] Finally we coupled the horizontal precipitation model to a dynamic vegetation model (IBIS). We initialized the coupled model (IBIS-HZP) with different landscapes, ones dominated by trees and others dominated by grassland. The different initial conditions had considerable effect on the equilibrium vegetation. Each simulation that was initialized with dominant tree cover yielded equilibrium vegetation that was dominated by trees, whereas in most of the simulations started with grassland, the equilibrium vegetation was dominated by grassland, except for one case. The equilibrium vegetation also depended considerably on cloud properties. For pristine clouds, the equilibrium vegetation would tend more to tree cover than for polluted ones. This implies that trees may or may not emerge from grassland, depending on the cloud properties. It is therefore important to obtain observations on cloud properties in Dhofar in the future.

[54] In conclusion, interaction of horizontal precipitation with canopy structure may, at least, considerably hamper reemergence of trees from grassland in a water limited cloud forest like the one in Dhofar. When trees are removed, the surface roughness is decreased and with it turbulent deposition of cloud droplets. Hence, total precipitation is decreased.

Less water is available at the surface for infiltration. These results indicate that reforestation efforts may need to be accompanied by irrigation to facilitate tree establishment. Once a canopy has formed and roughness of the surface has increased trees will be able to provide sufficient amount of water to sustain themselves.

[55] **Acknowledgments.** We thank the associate editor and two anonymous reviewers for their insightful comments and help improving this manuscript. Financial support for this research was provided by a grant from the Ministry of Regional Municipalities, Environment and Water Resources of the Sultanate of Oman and by a fellowship from the Martin Society of Fellows for Sustainability.

References

Bache, D. H. (1979), Particle-transport within plant canopies. 1. Framework for analysis, *Atmos. Environ.*, *13*, 1257–1262.

Beswick, K. M., K. J. Hargreaves, M. W. Gallagher, T. W. Choularton, and D. Fowler (1991), Size-resolved measurements of cloud droplet deposition velocity to a forest canopy using an eddy-correlation technique, *Q.J.R. Meteorol. Soc.*, *117*, 623–645.

Brook, G. A., and S.-W. Shen (2000), Rainfall in Oman and the United Arab Emirates: Cyclicity, influence of the Southern Oscillation and what the future may hold, *Arab World Geogr.*, *3*, 78–96.

Bubb, P., I. May, L. Miles, and J. Sayer (2004), *Cloud Forest Agenda*, UNEP-WCMC, Cambridge, UK.

Currie, R. I. (1992), Circulation and upwelling off the coast of south–east Arabia, *Oceanol. Acta*, *15*, 43–60.

del-Val, E., J. J. Armesto, O. Barbosa, D. A. Christie, A. G. Gutierrez, C. G. Jones, P. A. Marquet, and K. C. Weathers (2006), Rain forest islands in the Chilean semiarid region: Fog-dependency, ecosystem persistence and tree regeneration, *Ecosystems (N.Y., Print)*, *9*, 598–608.

Dollard, G. J., and M. H. Unsworth (1983), Field-measurements of turbulent fluxes of wind-driven fog drops to a grass surface, *Atmos. Environ.*, *17*, 775–780.

Eugster, W. (2006), Characteristics of fog and fogwater fluxes in a Puerto Rican elfin cloud forest, *Agric. For. Meteorol.*, *139*, 288–306.

Fallas, J. (2002), Net precipitation patterns in undisturbed and fragmented Costa Rica cloud forest, in *Proceedings to the Second International Colloquium, Hydrology and Water Management in the Tropics, Management in the Humid Tropics, Panama, 22–26 March 1999*, Int. Hydrolol. Programme, U.N. Educ., Sci., and Cult. Org., Paris.

Foley, J. A., I. C. Prentice, N. Ramankutty, S. Levis, D. Pollard, S. Sitch, and A. Haxeltine (1996), An integrated biosphere model of land surface processes, terrestrial carbon balance, and vegetation dynamics, *Global Biogeochem. Cycles*, *10*, 603–628.

Gallagher, M. W., K. Beswick, T. W. Choularton, H. Coe, D. Fowler, and K. Hargreaves (1992), Measurements and modeling of cloudwater deposition to moorland and forests, *Environ. Pollut.*, *75*, 97–107.

Gallagher, M. W., E. Nemitz, J. R. Dorsey, D. Fowler, M. A. Sutton, M. Flynn, and J. Duyzer (2002), Measurements and parameterizations of small aerosol deposition velocities to grassland, arable crops, and forest: Influence of surface roughness length on deposition, *J. Geophys. Res.*, *107*(D12), 4154, doi:10.1029/2001JD000817.

Hallberg, A. (1997), GCE: An overview, in *Cloud Multi-Phase Processes and High Alpine Air and Snow Chemistry*, edited by S. Fuzzi and D. Wagenbach, chap. 1, 286 pp., Springer, New York.

Hildebrandt, A. (2005) *Ecohydrology of a seasonal cloud forest in Dhofar*, 212 pp., Mass. Inst. of Technol, Cambridge.

Hildebrandt, A., and E. A. B. Eltahir (2006), Forest on the edge: Seasonal cloud forest in Oman creates its own ecological niche, *Geophys. Res. Lett.*, *33*, L11401, doi:10.1029/2006GL026022.

Hildebrandt, A., and E. A. B. Eltahir (2007), Ecohydrology of a seasonal cloud forest in Dhofar: 2. Role of clouds, soil type, and rooting depth in tree-grass competition, *Water Resour. Res.*, *43*, W11411, doi:10.1029/2006WR005262.

Hildebrandt, A., M. Al Aufi, M. Amerjeed, M. Shamas, and E. A. B. Eltahir (2007), Ecohydrology of a seasonal cloud forest in Dhofar: 1. Field experiment, *Water Resour. Res.*, *43*, W10411, doi:10.1029/2006WR005261.

Hutley, L. B., D. Doley, D. J. Yates, and A. Boonsaner (1997), Water balance of an Australian subtropical rainforest at altitude: The ecological and physiological significance of intercepted cloud and fog, *Aust. J. Bot.*, *45*, 311.

Juvik, J. O., and D. Nullet (1995), Relationship between rainfall, cloud-interception, and canopy throughfall in a Hawaiian montane forest, in *Tropical Montane Cloud Forests*, edited by L. S. Hamilton et al., Springer, New York.

Kucharik, C. J., J. A. Foley, C. Delire, V. A. Fisher, M. T. Coe, J. D. Lenters, C. Young-Molling, N. Ramankutty, J. M. Norman, and S. T. Gower (2000), Testing the performance of a dynamic global ecosystem model: Water balance, carbon balance, and vegetation structure, *Global Biogeochem. Cycles*, *14*, 795–825.

Kurschner, H., P. Hein, N. Kilian, and M. A. Hubaishan (2004), The Hybantho durae-Anogeissetum dhofaricae ass. nova-Phytosociology, structure and ecology of an endemic South Arabian forest community, *Phytocoenologia*, *34*, 569–612.

Lovett, G. M. (1984), Rates and mechanisms of cloud water deposition to a subalpine balsam fir forest, *Atmos. Environ.*, *18*, 361–371.

McFarquhar, G. M., and A. J. Heymsfield (2001), Parameterizations of INDOEX microphysical measurements and calculations of cloud susceptibility: Applications for climate studies, *J. Geophys. Res.*, *106*, 28,675–28,698.

Meister, J., M. A. Hubaishan, N. Kilian, and C. Oberprieler (2005), Chloroplast DNA variation in the shrub Justicia areysiana (Acanthaceae) endemic to the monsoon affected coastal mountains of the southern Arabian Peninsula, *Bot. J. Linn. Soc.*, *148*, 437–444.

Miller, G. M., and M. Morris (1988), *Plants of Dhofar, the southern region of Oman: Traditional, economic and medical uses, Off. of the Adviser for Conserv. of the Environ., Diwan of the Royal Court*, Sultanate of Oman, Muscat.

Nemitz, E., M. W. Gallagher, J. H. Duyzer, and D. Fowler (2002), Micrometeorological measurements of particle deposition velocities to moorland vegetation, *Q.J.R. Meteorol. Soc.*, *128*, 2281–2300.

Rogers, R. R., and M. K. Yau (1996), *A Short Course in Cloud Physics*, 3rd ed., 290 pp., Butterworth-Heinemann, Woburn, Mass.

Shi, W. (2000), The Oman upwelling zone during 1993, 1994 and 1995, *Deep Sea Res., Part II*, *47*, 1227–1247.

Shuttleworth, W. J. (1977), The exchange of wind driven fog and mist between vegetation and the atmosphere, *Boundary Layer Meteorol.*, *12*, 463–489.

Slinn, W. G. N. (1982), Predictions for particle deposition to vegetative canopies, *Atmos. Environ.*, *16*, 1785–1794.

Vermeulen, A. T., G. P. Wyers, F. G. Romer, N. F. M. VanLeeuwen, G. P. J. Draaijers, and J. W. Erisman (1997), Fog deposition on a coniferous forest in the Netherlands, *Atmos. Environ.*, *31*, 375–386.

Walmsley, J. L., R. S. Schemenauer, and H. A. Bridgman (1996), A method for estimating the hydrologic input from fog in mountains terrain, *J. Appl. Meteorol.*, *35*, 2237–2249.

Wieprecht, W., K. Acker, S. Mertes, J. Collett, W. Jaeschke, E. Bruggemann, D. Moller, and H. Herrmann (2005), Cloud physics and cloud water sampler comparison during FEBUKO, *Atmos. Environ.*, *39*, 4267–4277.

Zhang, L. M., S. L. Gong, J. Padro, and L. Barrie (2001), A size-segregated particle dry deposition scheme for an atmospheric aerosol module, *Atmos. Environ.*, *35*, 549–560.

E. A. B. Eltahir, Department of Civil and Environmental Engineering, Massachusetts Institute of Technology, 77 Massachusetts Avenue, Cambridge, MA 02139, USA.

A. Hildebrandt, Department of Computational Hydrosystems Leipzig, UFZ Helmholtz Centre for Environmental Research, Permoserstrasse 15, D-04318, Leipzig, Germany. (hildebra@alum.mit.edu)